SPATIALLY EXPLICIT SHALLOW LANDSLIDE SUSCEPTIBILITY MAPPING OVER LARGE AREAS

Dino BELLUGI[*, **], William E. DIETRICH[*], Jonathan STOCK[***], Jim McKEAN[****], Brian KAZIAN[*****] & Paul HARGROVE[******]

[*]Department of Earth & Planetary Science, University of California, Berkeley
[**]Department of Computational Science and Engineering, University of California, Berkeley
[***]United States Geological Survey, Menlo Park, California
[****]United States Forest Service, Rocky Mountain Research Station, Boise, Idaho
[*****]Intel Corporation, Santa Clara, California
[******]Lawrence Berkeley National Laboratory, Berkeley, California

ABSTRACT

Recent advances in downscaling climate model precipitation predictions now yield spatially explicit patterns of rainfall that could be used to estimate shallow landslide susceptibility over large areas. In California, the United States Geological Survey is exploring community emergency response to the possible effects of a very large simulated storm event and to do so it has generated downscaled precipitation maps for the storm. To predict the corresponding pattern of shallow landslide susceptibility across the state, we have used the model Shalstab (a coupled steady state runoff and infinite slope stability model) which susceptibility spatially explicit estimates of relative potential instability. Such slope stability models that include the effects of subsurface runoff on potentially destabilizing pore pressure evolution require water routing and hence the definition of upslope drainage area to each potential cell. To calculate drainage area efficiently over a large area we developed a parallel framework to scale-up Shalstab and specifically introduce a new efficient parallel drainage area algorithm which produces seamless results. The single seamless shallow landslide susceptibility map for all of California was accomplished in a short run time, and indicates that much larger areas can be efficiently modelled. As landslide maps generally over predict the extent of instability for any given storm. Local empirical data on the fraction of predicted unstable cells that failed for observed rainfall intensity can be used to specify the

likely extent of hazard for a given storm. This suggests that campaigns to collect local precipitation data and detailed shallow landslide location maps after major storms could be used to calibrate models and improve their use in hazard assessment for individual storms.

Key words: *shallow landslides, drainage area, slope stability, Shalstab, parallel computing*

INTRODUCTION

Downscaling of climate model precipitation predictions can now generate spatially detailed (i.e. at a scale of kilometres to tens of kilometres) maps of storm rainfall that include orographic and wind effects (e.g. Grell *et alii*, 1995; Giorgi *et alii*, 2001, Michalakes *et alii*, 2001; Widmann *et alii*, 2003; Salathé, 2003; Roe, 2005; Anders *et alii*, 2007; Dettinger *et alii,* in press). Such climate models typically operate over large areas (regional to continental to global). This allows an exploration of the effects of extreme storm events on hazard generation (through flooding and landsliding) and emergency response over these large areas. Landslides are always local, that is they are spatially discrete events, and from a management perspective the more spatially explicit the landslide susceptibility can be delineated, the more useful it is for planning. Gross maps based on threshold slopes derived from coarse grained digital elevation data (e.g. 30 m grid), for example, provide limited guidance. The increasing availability of higher resolution topographic

data (10m grid to 1 m (LiDAR-based)), the grid size of which approaches the scale of common shallow landslides (typically involving just the soil mantle), invites more mechanistic landslide models which have the potential to be broadly applicable. Such models, however, typically use hydrologic models to predict potential destabilizing pore pressure, and this means that drainage area to every cell must be determined. For small areas, this is readily accomplished, but for large areas (e.g. > 100 km^2 for 1 m data or 10,000 km^2 for 10 m data) conventional algorithms will not work efficiently because they cannot address the necessary amount of memory. This is because the computation of drainage area is a global operation (i.e. the information needed may theoretically come from any part of the landscape) and thus particularly challenging to implement seamlessly and efficiently.

Here we report the successful development of a parallel framework for large-scale spatially explicit landslide susceptibility assessment, and the implementation of an efficient seamless parallel drainage area algorithm. Our drainage area algorithm, available online at the National Center for Earth-surface Dynamics (http://www.nced.umn.edu/), is not dependent on the choice of landslide model and stands separately from its application to this problem.

This algorithm development was motivated by a challenge. As described in STOCK *et alii* (this volume), the United States Geological Survey (USGS) is conducting a study of the emergency preparedness in the state of California (414,000 km^2) for the effects of extreme storms. *Ar^kStorm*, their emergency-preparedness scenario, is intended to represent the most extreme storm events that have struck California (analogous those that devastated the state in 1861–62), as it is assumed such events will now increase in likelihood with global warming effects on climate. Recent work by DETTINGER *et alii* [in press] and RALPH *et alii* [2006] has illustrated that some of California's most damaging storms are atmospheric rivers of moisture that originate in the tropics and convey vast amounts of water vapour towards California in a narrow jet (e.g., 100-200 km wide) of moisture. When they strike California, these jets can deliver record rainfalls over the course of 1-3 days. Combining data from California's largest recent storms (1969 and 1985) DETTINGER *et alii* [in press] simulated an atmospheric river storm in a dynamic meteorological model (see http://meteora.ucsd.edu/

cap/arkstorm.html for details). They provided hourly rainfall simulation for all of California with resolution ranging from 2 to 6 km. The challenge here is can we predict shallow landslides across the entire state using the highest resolution state-wide topographic data (10m cells) and assess not only the potential location by the also the magnitude (number of landslides) for a given area given the predicted rainfall patterns.

There are many approaches for mapping shallow landslide potential across a landscape, ranging from purely empirical statistical approaches to process based models (e.g. review in CASADEI *et alii*, [2003]). There are insufficient studies in California to map the shallow landslide risk solely on statistical relationships. We elect as a first step in using the new drainage area algorithm to use the Shalstab model [MONTGOMERY & DIETRICH, 1994; DIETRICH *et alii*, 1995; DIETRICH *et alii*, 2001] which couples a steady state shallow subsurface flow model (to predict pore pressure distribution) with an infinite slope model. This model does not allow us to relate storm magnitude to landslide frequency, but its simplicity allows it to be applied across the entire state of California in the absence of spatially explicit data on such controlling factors as soil depth, root strength, soil saturated conductivity, and soil friction angle. Landslide susceptibility maps produced using the Shalstab model (or other hydrologically dynamic models), which successfully delineate areas of failure tend to also greatly over predict the extent of landsliding for a given storm event (e.g. CASADEI *et aii*., [2003]). Following Stock et al. [this volume] we suggest that this problem can be addressed empirically by relating the proportion of unstable cells that fail in a given storm to some measure of that storm magnitude

This first application of the slope stability model in a parallelized framework points to a need for systematic data collection on precipitation and landslide locations for a wide range of storms and across the diverse landscape found in a large area such as California. It is not clear to us at this point whether more mechanistic landslide models will be able to overcome the problem of over prediction and without considerable local calibration successfully delineate specific areas of instability for a given storm.

METHODS
TOPOGRAPHIC DATA

Basic topographic data for California were obtained from USGS's National Elevation Dataset (http://ned.usgs.gov/). The data are gridded at a resolution of 1/3 arc-second (approximately 10 m). Pre-processing consisted in assembling the data into larger tiles (1000 tiles, 972 km^2 each) and removing depressions using the standard ArcGis Fill tool. Depressions greater than 1.5 m were ignored, effectively preventing closed basins (e.g. Death Valley) from being filled. During the pre-processing steps the data were resampled at exactly 10m resolution, and saved in standard binary IEEE 32-bit floating point format for compatibility and efficiency.

SHALLOW LANDSLIDE SUSCEPTIBILITY MODEL

We adopted the widely used shallow landslide susceptibility model Shalstab [Montgomery and Dietrich, 1994; DIETRICH *et alii*, 1995; DIETRICH *et alii*, 2001] to estimate relative potential of shallow landslides initiated by storm rainfall. Shalstab couples a hydrological model to a limit-equilibrium slope stability model to calculate the critical steady-state rainfall necessary to trigger slope instability at any point in a landscape. Rainfall is assumed to infiltrate to a lower conductivity layer and flow along topographically determined paths above an impermeable layer. Under the simplifying assumption that soil transmissivity does not vary with depth, the degree of saturation of the soil profile can be written as

$$\frac{h}{z} = \frac{qa}{Tb\sin\theta} \tag{1}$$

where *h* (m) is the height of the saturated soil above the impermeable layer, *z* (m) is the total height of the soil, *q* (m/day) is the effective steady-state precipitation, *a* (m2)is the upslope drainage area, *b* (m)is the grid cell width, *T* (m^2/day) is the depth-integrated soil transmissivity and $^\theta$ (degrees) is the local slope. For the general (and conservative) case of cohesionless soils, the one-dimensional infinite slope stability model can be expressed as:

$$\rho_s gz\sin\theta\cos\theta = \left(\rho_s - \frac{h}{z}\rho_w\right)gz\cos^2\theta\tan\phi \tag{2}$$

where ρ_s and ρ_w are the bulk densities of soil and water, *z* is the soil thickness, $_g$ is gravity and φ is the

soil friction angle. Combining the two above equations we obtain the Shalstab equation in its simplest form:

$$\frac{q}{T} = \frac{b\sin\theta}{a}\left[\frac{\rho_s}{\rho_w}\left(1 - \frac{\tan\theta}{\tan\phi}\right)\right] \tag{3}$$

In essence, this model captures the topographic (i.e. area and slope) control on the spatial variability of pore pressures, and expresses the relative potential for shallow landsliding in terms of the ratio of the effective (steady-state) precipitation and the capability of the soil to conduct water, in a spatially explicit fashion. In this simple model, the only parameters are the friction angleφ , and the (saturated) soil bulk density ρ_s , which we set to values of 45 º and 1.7 g/cm^3, fairly typical of unconsolidated cohesionless soils.

Two important issues arise in the application of this model. The first is that mostly due to the hydrological simplifications, the model can not be linked to specific storm events The second is that as mentioned above, this model tends to over-predict the landsliding potential [DIETRICH *et alii*, 2001]. These issues point to the need for a calibration procedure discussed in a following section.

With respect to parallelization, it is important to note that computing the right hand side of equation (3) is a purely local operation: every grid cell has a local slope θ, and a drainage area a, both already assigned. This is what is referred to as an "embarrassingly parallel operation" [FOSTER, 1995], as no communication is required between any two cells. The computation of slope is performed on a 3 by 3 neighborhood, using a moving window. Communication in this case is required only when operating at the boundary of a processor's data domain. Thus, the real challenge for the parallelization of Shalstab lies entirely in the area computation, which is made possible by our new parallel algorithm.

PARALLEL FRAMEWORK

We utilize the Unified Parallel C (UPC) language [CARLSON, *et alii*, 1999], an extension of the C language based on the Partitioned Global Address Space (PGAS) parallel programming model. UPC offers programming abstractions similar to shared memory (where any process can read/write data allocated by another process), while allowing control over data layout that is critical to high performance and scalability [YELICK *et alii*, 2007]. UPC offers the program-

401

mers a seamless view of the data layer and a transparent communication layer (i.e. no explicit message passing is required), but data can be defined as local (i.e. near and reachable without communication costs) or as global (i.e. potentially far and more expensive to reach for improved efficiency. In particular, UPC allows for operations such as the slope computation discussed above to be simple to implement as well as efficient: the global address space allows for the transparent reference of an address outside of the local domain (in this case the boundary in the neighboring processor's domain), while the partitioning ensures that all memory access within a processor's domain is local. These characteristics make the language well suited for our application, where most computations are local but there is the need to obtain global information, as in the case of drainage area. The Lawrence Berkeley National Laboratory UPC compiler, used for this application, is now supported under many operating systems and architectures, and is freely available at http://upc.lbl.gov.

The parallel system used for testing and development is named Franklin, the National Energy Research Scientific Computing Center (NERSC)'s 38,288-CPU 2.3 GHz Opteron Cray XT-4 running a Linux-based operating system. It consists of 9572 quadprocessor nodes, each with 8GB of memory, interconnected with a high-speed SeaStar-2 network, and sharing a Lustre Parallel File System (LPFS) with 436Tb of user disk space. Theoretical peak performance is 9.2 GFlops/second per core, or 352TFlop/second for the whole system.

DRAINAGE AREA ALGORITHM

Generally, slope stability calculations, when implemented on a grid or a mesh, operate on information (such as topographic attributes) that is assigned to each cell, and thus are trivial to parallelize by using spatial domain decomposition of the (tiled) datasets [WILKINSON & ALLEN, 1999]. Most of the attributes that may be assigned to each grid cell (for example topographic slope) are also local in nature, requiring information only from pre-defined neighbourhoods of the target cell. Drainage area to a point, a fundamental landscape attribute, is defined as the total basin area above a specific point from which flow can reach such a point. The computation of drainage area is a global operation, as information is needed from all other
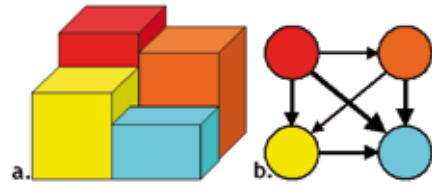

Fig.1 - *Idealized topography in 3-D view (a), and corresponding directed graph in plan view (b). Nodes correspond to grid cells and directed edges correspond to flow to downhill neighbours. Edge weights (illustrated here as edge thickness) correspond to the proportion of flow from outgoing cell. The upper-left node has no incoming edges and is a starting point for the algorithm. The lower-right node will be the last node to be processed.*

Fig. 2 - *Flow chart of initialization phase of the drainage area algorithm*

upstream tiles which may not be identifiable a priori. This presents a significant obstacle for parallelization, as it is not possible to determine a partitioning scheme for the grid such that communication and cross-thread dependencies are minimized during this computation. For this reason we develop a new efficient parallel drainage area algorithm.

The grid over which upslope area information must travel to each cell can be viewed as a connected directed graph [DASGUPTA *et alii*, 2006], with the nodes representing the grid cells and with edges representing flow from uphill to downhill neighbours (figure 1). The graph construction procedure comes at no cost, as it can be inserted in the flow direction and partitioning procedure that requires a complete pass over each grid cell. Pointers to nodes which have no incoming edges (corresponding to local maxima in the

402

5th International Conference on Debris-Flow Hazards Mitigation: Mechanics, Prediction and Assessment   Padua, Italy - 14-17 June 2011

Fig. 3   -   Flow chart of processing phase of the drainage area algorithm

elevation data), and the information they contain, are pushed into queues belonging to the thread that owns the downhill node (figure 2). The algorithm routes the drainage area information across this graph, operating only on nodes from the queues (i.e. nodes which have received all upslope information).

Individual threads poll the queues belonging to them, and remove the first item in the queue. The area information contained is then distributed to all the receiving node's downhill neighbours on the graph, according to the chosen flow weighting scheme. When information is sent across an edge of the graph, the edge is deleted. If, as a consequence of an edge deletion, a node no longer has any incoming edges, it becomes available for processing and it is placed onto the appropriate queue (figure 3). The algorithm terminates when the graph is fully disconnected, and all the queues are empty.

This algorithm is general, in other words it does not depend on the choice of flow partitioning. In our application we implement the multi-direction slope-dependent flow partitioning scheme, in which flow is distributed to all neighbouring downhill cells proportionately to the local slope [QUINN, *et alii*, 1991].

STORM INFLUENCE ON LANDSLIDES

Stock et al. [this volume] found an empirical rela-
tionship between a metric of rainfall and the fraction of unstable grid cells predicted by Shalstab that actually failed in historic storms (equation 1, Stock et al., this volume). This relationship accounts for the effect of rainfall intensity and duration on landslide abundance. They used digital landslide inventories mapped from air photographs taken after storms to construct storm-specific landslide catalogs for two southern California sites (Sunland and Santa Paula) and one northern California site (Montara). In the Santa Paula area they isolated landslides triggered by storms that occurred in 1969, 1998, 2001, and 2005; in the Sunland area they isolated landslides which occurred after storms in 1998 and 2005; in the Montara area they isolated landslides which occurred in 1955, 1982, and 2005.

Nearby rain gages recorded hourly rainfall data for all the storms of interest, with the exception of the 1955 and 1982 Montara storms (which were thus excluded from their study). Using the Santa Paula data as a training dataset, they found that the fraction of unstable cells that actually failed increased as a power law with the maximum 6-hour averaged rainfall intensity (unstable fraction = $0.00001 * I_{6-hr}^{2.7}$). The 1998 and 2005 Sunland events fell nicely on this curve (figure 6, Stock et al., this volume), suggesting that such a metric could be applied regionally. However, the 2005 Montara event in northern California had more than an order of magnitude lower fraction of unstable cells for similar 6-hour intensities. This points to the need for further region-specific calibration is needed if one wishes to apply such a method state wide.

STORM SIMULATION

Dettinger et al. [in press] simulated an atmospheric river storm *(Ar^kStorm)* combining data from two of California's most intense storms on record (January 1969 in southern California and February 1986 in northern California) as initial conditions in a spatially explicit dynamic meteorological model to describe a rapid sequence of several major storms over the state, yielding precipitation totals that go well beyond what actually occurred during the two separate events. They used a General Circulation Model (GCM) that depicts the world's climate over time at a coarse scale (hundreds of kilometres), coupling it over California with the state-of-the-art Weather Research and Forecast (WRF) model. WRF down-scales weather in a nested fashion down to a 2-km grid size, thus capturing the
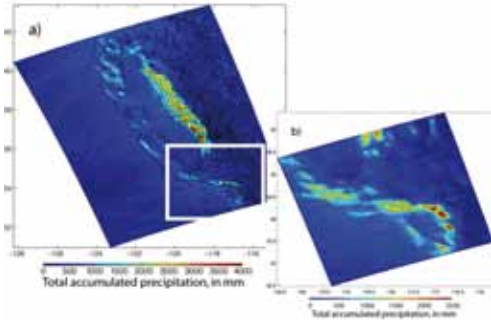
403

Fig. 4 - *Total accumulated precipitation during WRF simulation of ArkStorm scenario, in 6-km state-wide WRF nest (a), and 2-km southern California WRF nest (b). Notice that colour bars are not all the same; the domain of panel (b) is indicated by white rectangle in panel (a). Figure from Dettinger et al. [in press]*
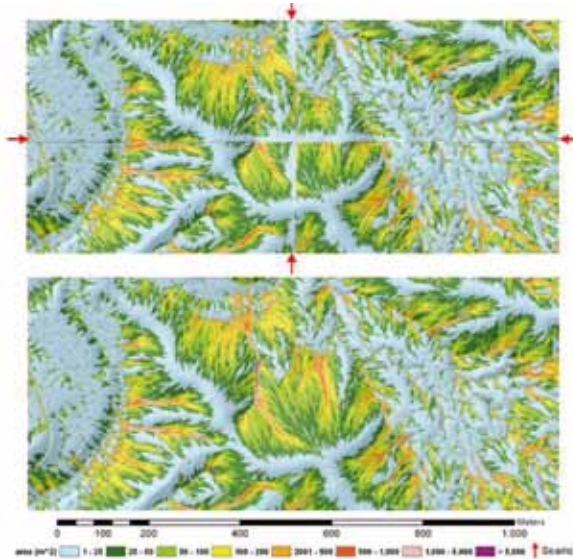

Category (*log(q/T)*)	Area (km²)	Percent (%)	Cum. Per. (%)
Uncond. Unstable	1,873.9	0.46	0.46
< -3.1	9,511.6	2.33	2.79
-2.8 to -3.1	10,758.8	2.63	5.42
-2.5 to -2.8	19,724.7	4.83	10.25
-2.2 to -2.5	23,078.2	5.65	15.90
-1.9 to -2.2	14,472.8	3.54	19.44
> -1.9	3,516.5	0.86	20.30
Uncond. Stable	325,724.7	79.70	100.00
Totals	408,661.2	100.00	

Tab 1 - *Distribution of Shalstab grid cells per stability class*

Fig. 5 - *Detail showing the intersection of four drainage area data tiles from a 1m LiDAR survey of the Eel River, CA (National Center for Airborne Laser Mapping). Panel (a) shows sequentially processed data tiles. The red arrows point to discontinuities in drainage area results. Panel (b) shows the same tiles processed by our parallel algorithm with a seamless grid*

relevant orographic and wind controls on precipitation. They provided hourly rainfall totals on a 2-km grid in southern California, and a 6-km grid over the whole state, effectively simulating the "perfect storm" scenario for the state of California (figure 4).

An example of the seamless drainage area computation resulting from the application of our parallel drainage area algorithm is shown in figure 5. The re-

sults of the application of the parallel Shalstab to the State of California are shown in figure 6. They are classified based on their q/T value (eq. 3), the ratio of effective steady-state precipitation and soil transmissivity required for instability. Two additional classes are also shown, representing areas having too low a gradient (unconditionally stable), and those with too high a gradient (unconditionally unstable). Table 1 illustrates the number of square kilometres and the percent area belonging to each class, for the entire state, reflecting the underlying distributions of steep and convergent areas. The results indicate that landslide susceptibility is generally focused in these steep convergent areas, and that while landslides pose a significant hazard in the state of California, the susceptible areas are a relatively small fraction of the entire landscape. For example, using a $log(q/T)$ threshold of -2.8, as suggested by Dietrich et al., 2001 (for 10m data), 5.42% of the landscape would be considered to be susceptible to shallow landsliding. Assuming a soil transmissivity value of 65 m²/day [Montgomery and Dietrich, 1994], a $log(q/T)$ threshold of -2.8 threshold would be equivalent to a critical rainfall rate of 103 mm/day.

The regression derived by Stock et al. [this volume], relating the fraction of unstable cells (calculated using our parallel Shalstab run), which may actually fail under the ArkStorm scenario, show that within the areas having similar lithology as the Santa Paula training site, the abundance of landslides under the ArkStorm scenario reflect the abundance of failures observed after the extreme winter storms of 1969.

All values of q/T above the "unconditionally stable" value were used by Stock et al. [this volume] to
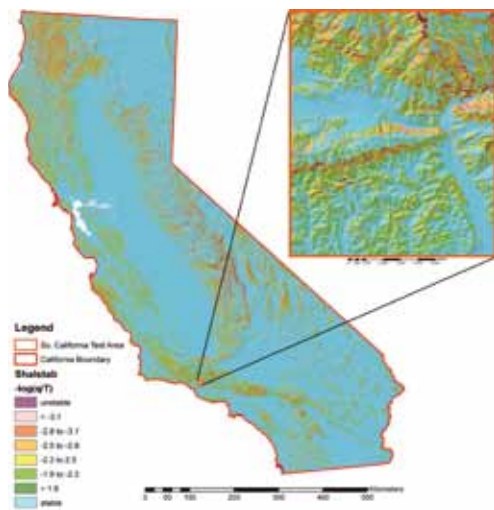
404

5th International Conference on Debris-Flow Hazards Mitigation: Mechanics, Prediction and Assessment   Padua, Italy - 14-17 June 2011

Fig. 6 - *Map showing Shalstab for the state of California. The inset map shows the Sunland test area southern California*

Fig. 7 - *Map showing potentially unstable areas for the state of California, as determined by a threshold of log(q/T) -2.8. The inset map shows the Sunland test area southern California*

delineate areas likely to fail in the storm. However, experience with Shalstab suggests that, when using 10m data, a *log(q/T)* threshold value of -2.8 will capture the vast majority of shallow landslide scars [DIETRICH *et alii*, 2001]. Figure 7 shows in red all the area of California that would be potentially unstable using this threshold.

DISCUSSION

Despite its simplicity, the application of Shalstab over the entire state of California at 10 m cell size required the development of a parallelized form of the drainage area determination for each cell. As topographic resolution increases further (from 10 m to 1 m data spacing) through airborne laser mapping, our ability to map landslides will greatly improve, but to make spatially explicit landslide predictions over large areas, parallelization of computation algorithms will be necessary. The largest area that a modern desktop computer can load into memory ranges from 100 km^2 for 1 m data to 10,000 km^2 for 10 m data. This implies that larger areas must be processed on a distributed memory architecture. Thus for seamless results over areas such as California, the only alternatives to parallelization are databases which are not practicable in terms of speed. Nevertheless, our scaling tests suggest that if we had 1 m data for all of California, even using all of the 9572 nodes available on Franklin (one of the world's most powerful computers) would still require several hours for Shalstab to run.

The STOCK *et alii* [this volume] findings suggest that a systematic effort be made across the state to collect local rainfall data and map landslide scars for specific storm events and then compute the proportion of failed to predicted cells for a given area. Different slope stability models could be used in such regressions. This approach has the advantage over the now widespread use of intensity-duration precipitation threshold plots for landsliding (e.g. ROSSI *et alii*, 2006; GUZZETTI *et alii*, 2008; BAUM & GODT, 2009) in providing estimates of the number of landslides in an area. Given the complex legacy of land use effects, uncertain fire history, and the presently unknown influence of bedrock type (and its tectonic history) there are good reasons to question whether this approach can be successful in general. Nonetheless, such data would prove invaluable in evaluating models and, hopefully, improving hazard prediction. Some simple steps can be taken to explore if improvements can be made in shallow landslide prediction at the state level using more mechanistic models. Data on soil thickness, vegetation cover, soil material properties, and geology (glaciated versus unglaciated) could be used to parameterize models that include root strength. Models that predict parameters such as soil depth (e.g. DIETRICH *et alii*, 1995) could exploit the parallelized framework and possibly improve estimates of the spatial structure of soil depth. Hydrologically dynamic

405

models which can route water and include the effects of vegetation at the spatial scale of DEM's (e.g. Wigmosta *et alii* 2002) could similarly exploit the parallelized framework and improve the spatial structure of the pore pressure field.

CONCLUSION

Detailed precipitation predictions now available at the large scale allow and invite the assessment of the effects of extreme storm parallel version of Shalstab allow for fast seamless results even when applied to large areas. We applied the algorithms to the state of California (414,000 km²) using 10 m resolution topographic data, but tests show that our application could process in a few hours all of the United States (9,830,000 km²) or all of Europe (10,180,000 km²) with similar data resolution.

To contribute to the USGS ArkStorm emergency preparedness study we ran Shalstab for the entire state. The extent of landsliding for any given storm will be greatly over-predicted by this model. Empirical relationships between the percent of predicted unstable

cells that failed for a given storm are needed to estimate the magnitude of the landslide response. We anticipate that higher resolution topographic data, more mechanistic models, and increased computational efficiency through parallelization algorithms will progressively improve shallow landslide hazard predictions

REFERENCES

Anders A.M., Roe G.H., Durran D.R. & Minder J.R. (2007) - *Small- Scale Spatial Gradients in Climatological Precipitation on the Olympic Peninsula.* J. Hydrometeor, **8:** 1068–1081.

Baum R.L. & Godt J.W. (2009) - *Early warning of rainfall-induced shallow landslides and debris flows in the USA.* Landslides. doi:10.1007/s10346-009-0177-0

Carlson W., Draper J.M., Culler D.E., Yelick K., Brooks E. & Warren K. (1999) - *Introduction to UPC and Language Specification*

Casadei M., Dietrich W. E. & Miller N.L. (2003) - *Testing a model for predicting the timing and location of shallow landslide initiation in soil mantled landscapes.* Earth Surface Processes and Landforms, **28:** 925-950.

Dasgupta S., Papadimitriou C.H.,& Vazirani U.V. (2006) - *Algorithms.* McGraw-Hill Higher Education.

Dettinger M.D., Ralph F.M., Hughes M., Das T., Neiman P., Cox D., Estes G., Reynolds D., Hartman R., Cayan D. & Jones L. (in press). *Requirements and designs for a winter storm scenario for emergency preparedness and planning exercises in California.*

Dietrich W .E., Reiss R., Hsu M. & Montgomery D.R. (1995) - *A process-based model for colluvial soil depth and shallow landsliding using digital elevation data.* Hydrological Processes, **9:** 383-400.

Dietrich W.E., Bellugi D., & Real de Asua R. (2001) - *Validation of the shallow landslide model, SHALSTAB, for forest management, in M..S. Wigmosta, and S. J. Burges, editors, Land Use and Watersheds:* Human influence on hydrology and geomorphology in urban and forest areas, Amer. Geoph. Union, Water Science and Application, **2:** 195-227.

Foster I. (1995) - *Designing and building parallel programs*, Addison-Wesley.

Giorgi F., Hewitson B., Christensen J., Fu C., Hulme M., Mearns L., von Storch H., Whetton P. *et alii* (2001) - *Regional climate simulation - evaluation and projections.* In Climate Change 2001: The Scientific Basis, Houghton J.T., Ding Y., Griggs D.J., Nigmer M., van der Linslen P.J., Dai X. (eds). Cambridge University Press.

Grell G.A., Dudhia J. & Stauffer D.R. (1995) - *A description of the fifthgeneration Penn State NCAR Mesoscale Model (MM5).* NCAR Tech. Note TN-398 + STR. 122 pp.

Guzzetti F., Peruccacci S., Rossi M. & Stark C.P. (2008) - *The rainfall intensity–duration control of shallow landslides and debris flows: an update.* Landslides. **5**(1)**:** 3-17.

406

5th International Conference on Debris-Flow Hazards Mitigation: Mechanics, Prediction and Assessment   *Padua, Italy - 14-17 June 2011*

Michalakes J., Chen S., Dudhia J., Hart L., Klemp J., Middlecoff J. & Skamarock W. (2001) - *Development of a next generation regional weather research and forecast model*. Developments in Teracomputing: Proceedings of the Ninth ECMWF Workshop on the Use of High Performance Computing in Meteorology, W. Zwieflhofer and N. Kreitz, Eds., World Scientific, 269–276.

Montgomery D.R. & Dietrich W.E. (1994) - *A physically-based model for topographic control on shallow landsliding,* Water Resources Research, **30**(4): 1153-1171.

Quinn P., Beaven K., Chevallier P. & Planchon O. (1991) - *The prediction of hillslope flow for distributed hydrological modeling using digital terrain models.* Hydrological processes, **5**: 59-79.

Ralph F.M., Neiman P.J., Wick G.A., Gutman S.I., Dettinger M.D., Cayan D.R. & White A.B. (2006) - *Flooding on California's Russian River: Role of atmospheric rivers*. Geophys. Res. Lett., **33**, L13801, doi:10.1029/2006GL026689.

Roe G.H. (2005) - *Orographic precipitation.* Annual Review of Earth and Planetary Sciences, **33**: 645–671.

Rossi M., Peruccacci S. & Guzzetti F. (2006) - *A review of rainfall thresholds for the initiation of landslides.* Geophys Res Abstr. **8**: 02323.

Salathé E.P. (2003) - *Comparison of various precipitation downscaling methods for the simulation of streamflow in a rain-shadow river basin*. International Journal of Climatology, **23:** 887-901. doi: 10.1002/joc.922

Stock, J.D. & Bellugi D. (this volume) - *An empirical method to forecast the effect of storm intensity on shallow landslide abundance.* Proceedings of the 5th International Conference on Debris-Flow Hazards Mitigation: Mechanics, Prediction and Assessment, Italian Journal of Engineering Geology and Environment.

Widmann M., C.S. Bretherton, E.P. Salathé, 2003, *Statistical Precipitation Downscaling over the Northwestern United States Using Numerically Simulated Precipitation as a Predictor.* J. Climate, **16:**799–816.

Wigmosta M.S., Nijssen B., Storck P. & Lettenmaier D.P. (2002) - *The Distributed Hydrology Soil Vegetation Model, In-Mathematical Models of Small Watershed.* Hydrology and Applications, Singh V.P. & Frevert D.K., eds., Water Resource Publications, Littleton, CO.: 7-42.

Wilkinson B. & Allen C.M. (1999) - *Parallel Programming*, Prentice- Hall.

Yelick K., Bonachea D., Chen W., Colella P., Datta K., Duell J., Graham S.L., Hargrove P., Hilfinger P., Husbands P., Iancu C., Kamil A., Nishtala R., Su J., Welcome M. & Wen T. (2007) - *Productivity and performance using partitioned global address space languages.* In Proceedings of the 2007 international Workshop on Parallel Symbolic Computation (London, Ontario, Canada, July 27 - 28, 2007). PASCO '07. ACM, New York, NY, 24-32.